Two-photon absorption with tightly focused optical vortices

Forbes, Kayn, Green, Dale

SPIE.

Two-photon absorption with tightly focused optical vortices

Kayn A. Forbes* and Dale Green

School of Chemistry, University of East Anglia, Norwich NR4 7TJ, United Kingdom

*k.forbes@uea.ac.uk

ABSTRACT

Unlike single photon absorption, the rate of multiphoton absorption processes is dependent on the polarization state of the exciting optical field. Multiphoton absorption spectroscopy is predominantly carried out with an exciting light source which is structured and polarized in a 2D sense in the transverse (x,y) plane, but homogeneous along the direction of propagation (z). Here we study two-photon absorption (TPA) with tightly focused optical vortices, where the spatial confinement generates significant longitudinal components of the electromagnetic fields in the direction of propagation, producing a 3D structured optical field at the focal plane. We discover that the additional polarization degree of freedom in the z direction for 3D structured light produces novel results in TPA compared to the preceding paraxial source excitation.

Keywords: Structured light, nonlinear spectroscopy, optical spectroscopy, nonlinear optics, optical vortex, multiphoton absorption

1. INTRODUCTION

Multiphoton absorption processes are nonlinear optical interactions which have found widespread application[1]. In particular, two photon absorption (TPA), has been widely utilized in a range of distinct areas such as non-invasive fluorescence microscopy and semiconductor photonics[2–4]. Advantages include: TPA requires lower energy photons to probe transitions; TPA possesses a different set of selection rules compared to single photon absorption; and also compared to single photon absorption, TPA is dependent on the polarization state of the exciting beam, even for isotropic material samples. It is this latter property of TPA which has inspired the work in this paper concerning the TPA mechanism for tightly focused structured laser beams. Propagating plane waves and paraxial laser sources have polarization degrees of freedom which are transverse to the direction of propagation z and are homogenous along z. As such, we may refer to these beams as being 2D structured and polarized in the 2D (x,y) sense[5]. However, spatially confining optical fields gives rise to longitudinal electromagnetic fields in the direction of propagation z, and we call light which is inhomogeneous along its direction of propagation '3D structured light'. An important type of structured light are optical vortex modes due to their spectacular implementation in a diverse range of areas[6] since the pioneering work of Les Allen et al. in 1992[7]. Their distinguishing feature is that they propagate with the helical phase factor $\exp(i\ell\phi)$ where $\ell \in \mathbb{Z}$, and convey an orbital angular momentum (OAM) of $\ell\hbar\hat{z}$ per photon. In this work we look specifically at the TPA by molecular matter of 3D structured optical vortices.

2. QED THEORY OF TPA

We use the Power-Zineau-Woolley (PZW) formulation of non-relativistic quantum electrodynamics (QED), which casts the Hamiltonian operator describing the interaction between the radiation and matter present in the system in terms of the electromagnetic fields coupling to the multipolar transition moments of the material[8,9]:

$$H_{\text{int}}(\xi) = -\varepsilon_0^{-1}\mu_i(\xi)d_i^{\perp}(\boldsymbol{R}_{\xi}) - ...\text{h.o.t.}, \tag{1}$$

where $\boldsymbol{\mu}(\xi)$ is the electric dipole transition moment operator and $\boldsymbol{d}^{\perp}(\boldsymbol{R}_{\xi})$ is the electric displacement field operators (transverse to the Poynting vector); we use standard suffix notation for tensor quantities and imply the Einstein summation convention for repeated indices throughout (i.e. $a_i b_i = \boldsymbol{a} \cdot \boldsymbol{b}$). The interaction Hamiltonian (1) describes the electric-dipole (E1) coupling, and in the vast majority of optical interactions it is the dominant form of interaction and truncating (1) (ignoring the higher order terms (h.o.t.)) to only including this E1 coupling is the electric-dipole approximation. We work within this E1 approximation throughout this work, though the general theory produced here can easily account for the higher-order couplings.

We consider a system that is comprised of a single laser beam of n photons of the single mode (k, η, ℓ, p) incident upon a collection of N particles ξ. The initial $|I\rangle$ and final $|F\rangle$ states of this system for TPA from a single beam are thus

$$|I\rangle = |n(k, \eta, \ell, p)\rangle \prod_{\xi}^{N} |E_0(\xi)\rangle; \quad |F\rangle = |(n-2)(k, \eta, \ell, p)\rangle |E_m(\xi')\rangle \prod_{\xi' \neq \xi}^{N} |E_0(\xi)\rangle. \tag{2}$$

Because TPA is a second-order process with respect to H_{int} we require second-order pertubation theory in order to calculate the matrix element M_{FI} of TPA [10]

$$M_{FI} = \sum_r \langle (n-2)(k, \ell, p); E_m | -\varepsilon_0^{-1}\boldsymbol{\mu}(\xi) \cdot \boldsymbol{d}^{\perp}(\boldsymbol{R}_{\xi}) | E_r; (n-1)(k, \ell, p)\rangle$$
$$\times \langle (n-1)(k, \ell, p); E_r | -\varepsilon_0^{-1}\boldsymbol{\mu}(\xi) \cdot \boldsymbol{d}^{\perp}(\boldsymbol{R}_{\xi}) | E_0; n(k, \ell, p)\rangle \frac{1}{E_0 - E_r + \hbar\omega}. \tag{3}$$

As mentioned in the Introduction, we refer to light as being 2D structured if it is inhomogeneous in the transverse plane (x,y) but is homogenous along the direction of propagation (z)[5]. Examples of 2D structured optical fields would be paraxial optical vortices (phase structured) or vector beams (polarization structured). 3D structured light manifests when an optical field is spatially confined, examples include evanescent waves or tightly focussed laser beams. The key physical property of 3D structured light fields, that which is responsible for much of their extraordinary properties, is the fact they exhibit longitudinal (with respect to the direction of propagation) electromagnetic field components. The magnitude of longitudinal fields is proportional to a smallness parameter, in the case of focused laser beams it is $(\lambda / 2\pi w_0)^{-1}$, and under very tight focusing they can even exceed transverse field components. The QED electric displacement field operator $\boldsymbol{d}^{\perp}(\boldsymbol{r})$ (the superscript denotes transversality with respect to the Poynting vector) for an arbitrarily 2D-polarized 3D Laguerre Gaussian (LG) mode, $e_i^{(\eta)}(k\hat{z})$ being the polarization unit vector, is given as[11]

$$d_i^{\perp}(\boldsymbol{r}) = i \sum_{k,\eta,\ell,p} \left(\frac{\hbar c k \varepsilon_0}{2 A_{\ell,p}^2 V} \right)^{1/2} \left[\left\{ e_i^{(\eta)}(k\hat{z}) + \frac{i}{k}\hat{z}_i \left(\frac{\partial}{\partial x} + \frac{\partial}{\partial y} \right) \right\} \right.$$

$$\left. f_{|\ell|,p}(r) a_{|\ell|,p}^{(\eta)}(k\hat{z}) e^{i(kz+\ell\phi)} - \text{H.c.} \right], \tag{4}$$

where $k = 2\pi/\lambda$ is the wavenumber, V is a quantization volume, $A_{\ell,p}^2$ is a normalization constant for LG modes, $\sigma = \pm 1$, the positive sign designates left-handed circularly polarized light (CPL); the negative sign right-handed CPL, $a_{|\ell|,p}^{(\sigma)}(k\hat{z})$ is the annihilation operator, $\exp i(kz + \ell\phi)$ is the phase, $\ell \in \mathbb{Z}$ is the topological charge, H.c. stands for Hermitian conjugate, and $f_{|\ell|,p}(r)$ is the radial distribution function around the focal plane

$$f_{|\ell|,p}(r) = \frac{C_p^{|\ell|}}{w_0} \left(\frac{\sqrt{2}r}{w_0} \right)^{|\ell|} e^{-\frac{r^2}{w_0^2}} L_p^{|\ell|} \left[\frac{2r^2}{w_0^2} \right], \tag{5}$$

where w_0 is the beam waist, the normalization constant is given by $C_p^{|\ell|} = \sqrt{2p!/\left[\pi \left(p + |\ell| \right)! \right]}$ and $L_p^{|\ell|}$ is the generalised Laguerre polynomial of order p.

3. LINEAR POLARIZATION 3D LG TPA

Using (4) in (1) and inputting the interaction Hamiltonian operator into (3) gives the matrix element for TPA for a 2D-linearly polarized (in the x direction) 3D LG mode as

$$M_{fi} = \left(\frac{\hbar c k}{4\varepsilon_0 A_{\ell,p}^2 V} \right) \sqrt{n} \sqrt{n-1} \left(e_i^{(x)} e_j^{(x)} f^2 + e_i^{(x)} \hat{z}_j \frac{i}{k} \beta f + \hat{z}_i e_j^{(x)} \frac{i}{k} \beta f - \hat{z}_i \hat{z}_j \frac{1}{k^2} \beta^2 \right) e^{2i\ell\phi} e^{2ikz} \alpha_{ij}^{m0}, \tag{6}$$

where most notational dependencies have been suppressed for clarity and we have defined $\left[(\cos\phi) f_{|\ell|,p}'(r) - \frac{i\ell}{r}(\sin\phi) f_{|\ell|,p}(r) \right] = \beta$ and $\alpha_{ij}^{m0}(\xi,\omega,\omega)$ is the well-known dynamic molecular polarizability tensor

$$\alpha_{ij}^{m0}(\xi,\pm\omega,\pm\omega) = -\sum_r \frac{\langle m|\mu_i(\xi)|r\rangle\langle r|\mu_j(\xi)|0\rangle}{E_0 - E_r + \hbar\omega} - \frac{\langle m|\mu_j(\xi)|r\rangle\langle r|\mu_i(\xi)|0\rangle}{E_0 - E_r + \hbar\omega}$$

$$= \sum_r \frac{\mu_i^{mr}(\xi)\mu_j^{r0}(\xi)}{E_{r0} \mp \hbar\omega} + \frac{\mu_j^{mr}(\xi)\mu_i^{r0}(\xi)}{E_{r0} \mp \hbar\omega}. \tag{7}$$

The rate Γ of TPA can be calculated as (where we ignore constants and factors in the Fermi golden rule which don't alter the physics we are interested in)

$$\Gamma \propto \sum_{\xi} \left| M_{fi}(\xi) \right|^2$$

$$= N \frac{\overline{I}^2 g^{(2)}}{16\varepsilon_0^2 c^2} \left[\left(e_i e_j f^2 + e_i \hat{z}_j f \frac{i}{k} \beta + \hat{z}_i e_j^{(x)} \frac{i}{k} \beta f - \hat{z}_i \hat{z}_j \frac{1}{k^2} \beta^2 \right) \right.$$

$$\left. \times \left(\overline{e}_k \overline{e}_l f^2 - \overline{e}_k \hat{z}_l f \frac{i}{k} \overline{\beta} - \hat{z}_k \overline{e}_l f \frac{i}{k} \overline{\beta} - \hat{z}_k \hat{z}_l \frac{1}{k^2} \overline{\beta}^2 \right) \right] \alpha_{ij}^{m0} \overline{\alpha}_{kl}^{m0}, \tag{8}$$

$\overline{I} = \langle n \rangle \hbar c^2 k \big/ A_{|\ell|,p}^2 V$ is the mean beam intensity, $g^{(2)} = \langle n(n-1) \rangle \big/ \langle n \rangle^2$ is the degree of second-order coherence, and N is the number of absorbers. As it stands, (8) is applicable to particles which have a specific orientation. In order to make (8) applicable to randomly oriented particles – such as those in liquids or gases – we require the rotational average of (8). Using standard methods[12] for the fourth-rank material tensor average $\langle \alpha_{ij} \overline{\alpha}_{kl} \rangle$ we produce the rate for orientationally averaged particles:

$$\langle \Gamma \rangle \propto N \frac{\overline{I}^2 g^{(2)}}{16\varepsilon_0^2 c^2} \frac{1}{15} \left[\left(\alpha_{\lambda\lambda}^{m0} \overline{\alpha}_{\mu\mu}^{m0} + \alpha_{\lambda\mu}^{m0} \overline{\alpha}_{\lambda\mu}^{m0} + \alpha_{\lambda\mu}^{m0} \overline{\alpha}_{\mu\lambda}^{m0} \right) f^4 \right.$$

$$- \left(4\alpha_{\lambda\lambda}^{m0} \overline{\alpha}_{\mu\mu}^{m0} - \alpha_{\lambda\mu}^{m0} \overline{\alpha}_{\lambda\mu}^{m0} - \alpha_{\lambda\mu}^{m0} \overline{\alpha}_{\mu\lambda}^{m0} \right) \mathrm{Re} \frac{1}{k^2} f^2 \beta^2$$

$$+ \left(-2\alpha_{\lambda\lambda}^{m0} \overline{\alpha}_{\mu\mu}^{m0} + 3\alpha_{\lambda\mu}^{m0} \overline{\alpha}_{\lambda\mu}^{m0} + 3\alpha_{\lambda\mu}^{m0} \overline{\alpha}_{\mu\lambda}^{m0} \right) f^2 \frac{1}{k^2} |\beta|^2$$

$$\left. + \left(\alpha_{\lambda\lambda}^{m0} \overline{\alpha}_{\mu\mu}^{m0} + \alpha_{\lambda\mu}^{m0} \overline{\alpha}_{\lambda\mu}^{m0} + \alpha_{\lambda\mu}^{m0} \overline{\alpha}_{\mu\lambda}^{m0} \right) \frac{1}{k^4} \beta^2 \overline{\beta}^2 \right]. \tag{9}$$

Invoking the full Fermi golden rule, we can write the key part of the result in terms of the factor $B_{\mathrm{LG(lin)}}^{(2)}$: the two-photon analogue of the Einstein B-coefficient[10]

$$B_{\mathrm{3D\text{-}LG(lin)}}^{(2)} = \frac{1}{240\hbar^2 c\varepsilon_0^2} \left[\left(\alpha_{\lambda\lambda}^{m0} \overline{\alpha}_{\mu\mu}^{m0} + \alpha_{\lambda\mu}^{m0} \overline{\alpha}_{\lambda\mu}^{m0} + \alpha_{\lambda\mu}^{m0} \overline{\alpha}_{\mu\lambda}^{m0} \right) f^4 \right.$$

$$- \left(4\alpha_{\lambda\lambda}^{m0} \overline{\alpha}_{\mu\mu}^{m0} - \alpha_{\lambda\mu}^{m0} \overline{\alpha}_{\lambda\mu}^{m0} - \alpha_{\lambda\mu}^{m0} \overline{\alpha}_{\mu\lambda}^{m0} \right) A$$

$$+ \left(-2\alpha_{\lambda\lambda}^{m0} \overline{\alpha}_{\mu\mu}^{m0} + 3\alpha_{\lambda\mu}^{m0} \overline{\alpha}_{\lambda\mu}^{m0} + 3\alpha_{\lambda\mu}^{m0} \overline{\alpha}_{\mu\lambda}^{m0} \right) B$$

$$\left. + \left(\alpha_{\lambda\lambda}^{m0} \overline{\alpha}_{\mu\mu}^{m0} + \alpha_{\lambda\mu}^{m0} \overline{\alpha}_{\lambda\mu}^{m0} + \alpha_{\lambda\mu}^{m0} \overline{\alpha}_{\mu\lambda}^{m0} \right) C \right], \tag{10}$$

A, B, and *C*, are shorthand and their explicit expressions are shown in Table 1.

Label	Factor
A	$\operatorname{Re}\dfrac{1}{k^2}f^2\beta^2$
B	$f^2\dfrac{1}{k^2}\lvert\beta\rvert^2$
C	$\dfrac{1}{k^4}\beta^2\overline{\beta}^2$
D	$\dfrac{1}{k^2}f^2\ \chi^2$
E	$\dfrac{1}{2k^4}\chi^4$

Table 1: Optical factors relating to the shorthand notation A-E.

The symmetry properties of the α tensor may be analysed by a decomposition into irreducible components which, with the aid of character tables, provide knowledge on selection rules and forbidden transitions in specific molecules. In general we can use the following to decompose the tensor into weight 0 (scalar), weight 1 (antisymmetric), and weight 2 (symmetric) via[13]

$$\alpha_{\lambda\lambda}\overline{\alpha}_{\mu\mu} = 3\alpha_{\lambda\mu}^{(0)}\overline{\alpha}_{\lambda\mu}^{(0)} = \alpha_{\lambda\lambda}^{(0)}\overline{\alpha}_{\mu\mu}^{(0)}$$
$$\alpha_{\lambda\mu}\overline{\alpha}_{\lambda\mu} = \alpha_{\lambda\mu}^{(0)}\overline{\alpha}_{\lambda\mu}^{(0)} + \alpha_{\lambda\mu}^{(1)}\overline{\alpha}_{\lambda\mu}^{(1)} + \alpha_{\lambda\mu}^{(2)}\overline{\alpha}_{\lambda\mu}^{(2)}$$
$$\alpha_{\lambda\mu}\overline{\alpha}_{\mu\lambda} = \alpha_{\lambda\mu}^{(0)}\overline{\alpha}_{\mu\lambda}^{(0)} + \alpha_{\lambda\mu}^{(1)}\overline{\alpha}_{\mu\lambda}^{(1)} + \alpha_{\lambda\mu}^{(2)}\overline{\alpha}_{\mu\lambda}^{(2)}$$
$$= \alpha_{\lambda\mu}^{(0)}\overline{\alpha}_{\lambda\mu}^{(0)} - \alpha_{\lambda\mu}^{(1)}\overline{\alpha}_{\lambda\mu}^{(1)} + \alpha_{\lambda\mu}^{(2)}\overline{\alpha}_{\lambda\mu}^{(2)}. \tag{11}$$

This allows (10) to be written in terms of irreducible components as

$$B_{\text{3D-LG(lin)}}^{(2)} = \frac{1}{240\hbar^2 c\varepsilon_0^2}\left[\left(f^4 - 2A + C\right)\frac{5}{3}\alpha_{\lambda\lambda}^{(0)}\overline{\alpha}_{\mu\mu}^{(0)}.\right.$$
$$\left.\left(f^4 + A + 3B + C\right)2\alpha_{\lambda\mu}^{(2)}\overline{\alpha}_{\lambda\mu}^{(2)}\right]. \tag{12}$$
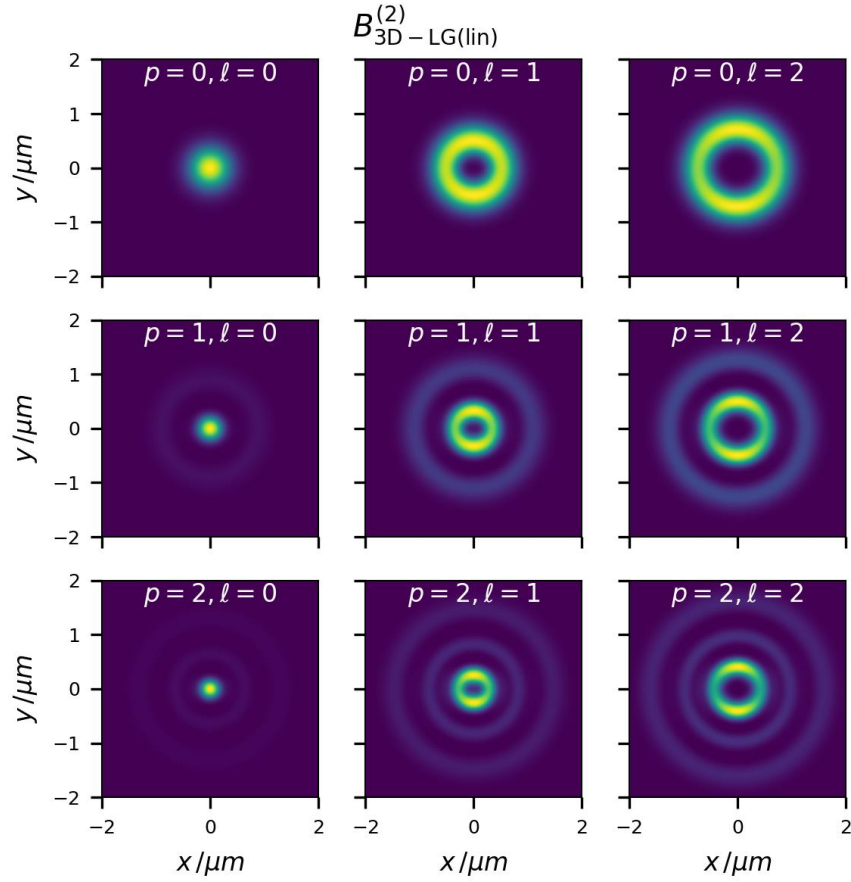
$$B^{(2)}_{3D-LG(lin)}$$

Figure 1: Equation (10) for different modes (ℓ, p) where $w_0 = \lambda$.

It is illuminating to compare the TPA Einstein *B*-coefficient $B^{(2)}_{3D\text{-}LG(lin)}$ (12) to that of a paraxial (well-collimated) 2D-linearly polarized 2D LG 2D-LG(lin):

$$B^{(2)}_{2D\text{-}LG(lin)} = \frac{1}{240\hbar^2 c\varepsilon_0^2}\left[\frac{5}{3}\alpha^{(0)}_{\lambda\lambda}\bar{\alpha}^{(0)}_{\mu\mu} + 2\alpha^{(2)}_{\lambda\mu}\bar{\alpha}^{(2)}_{\lambda\mu}\right]f^4_{|\ell|,p}. \tag{13}$$

The TPA Einstein *B*-coefficient (13) is essentially the result for plane wave TPA[10]. Figure 2 compares (12) to (13) and what we see is that the 3D structured focal field produced by a tightly focused linearly polarized 2D LG mode does not significantly influence the relative contributions of scalar weight 0 and symmetric weight 2 TPA when compared to a plane wave excitation, except in the case of $\ell = 1$ where there are discernible on-axis contributions to both weights 0 and 2 in the 3D structured field case.
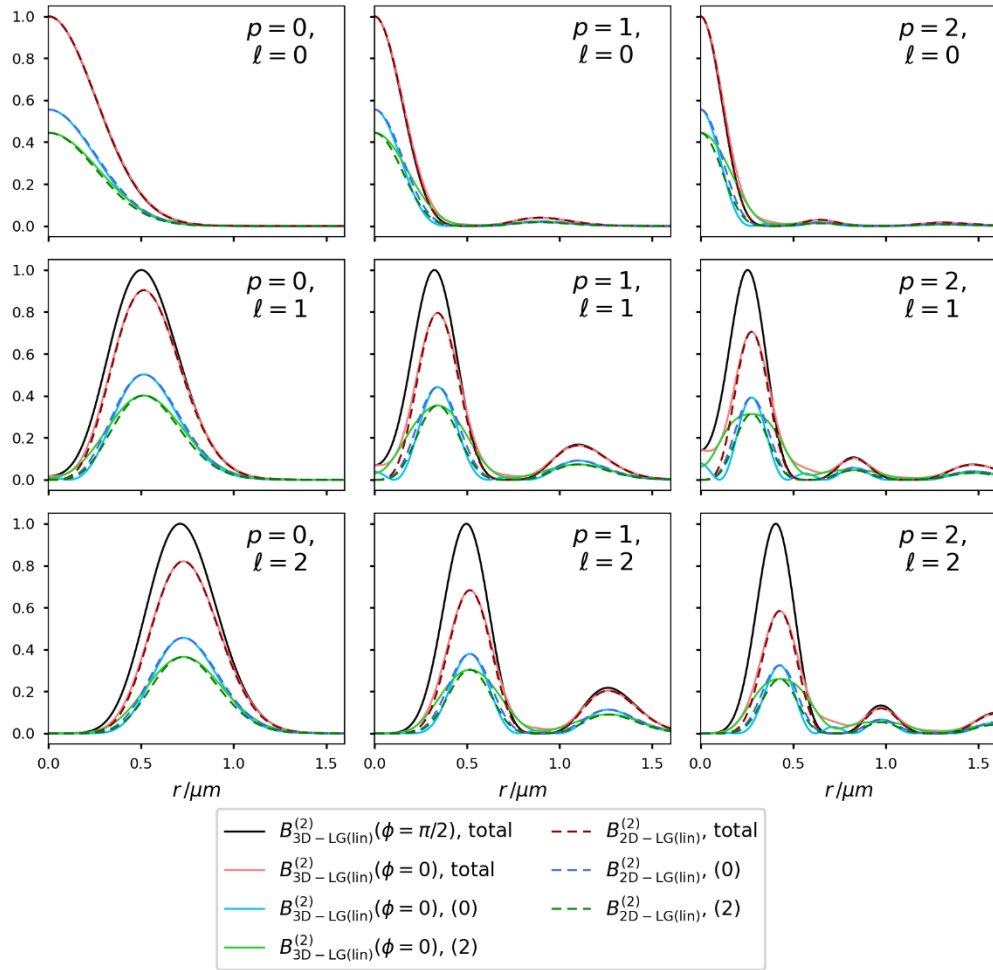
Figure 2: Irreducible tensor analysis of 3D LG mode TPA (12) (solid lines) versus 2D LG mode (13) (dashed lines). $w_0 = \lambda$.

4. CIRCULARLY POLARIZED 3D LG TPA

The matrix element for TPA of a 2D-circularly polarized 3D LG mode is,

$$
\begin{aligned}
M_{FI} = \left(\frac{\hbar c k}{4\varepsilon_0 V} \right) \left(n\{n-1\} \right)^{1/2} &\left[e_i^{(\sigma)} e_j^{(\sigma)} f^2 + e_j^{(\sigma)} \hat{z}_i f \frac{i}{\sqrt{2}k} \chi e^{i\sigma\phi} \right. \\
&\left. + e_i^{(\sigma)} \hat{z}_j f \frac{i}{\sqrt{2}k} \chi e^{i\sigma\phi} - \hat{z}_i \hat{z}_j \frac{1}{2k^2} \chi^2 e^{2i\sigma\phi} \right] e^{2i\ell\phi} e^{2ikz} \alpha_{ij}^{m0},
\end{aligned}
\tag{14}
$$

where we introduce the shorthand notation $\chi = f'_{|\ell|,p}(r) - \ell\sigma\dfrac{1}{r}f_{|\ell|,p}(r)$. In contrast to the linear case, carrying out the

average of the rate of (14) we have less terms to deal with because $e \cdot e = 0$ and $\bar{e} \cdot \bar{e} = 0$ for circular polarizations. The rotationally averaged rate is

$$\langle\Gamma\rangle \propto N\frac{\bar{I}^2 g^{(2)}}{16\varepsilon_0^2 c^2}\frac{1}{30}\Big[\Big[\Big(-2\alpha_{\lambda\lambda}^{m0}\bar{\alpha}_{\mu\mu}^{m0} + 3\alpha_{\lambda\mu}^{m0}\bar{\alpha}_{\lambda\mu}^{m0} + 3\alpha_{\lambda\mu}^{m0}\bar{\alpha}_{\mu\lambda}^{m0}\Big)f^4.$$
$$+\Big(-2\alpha_{\lambda\lambda}^{m0}\bar{\alpha}_{\mu\mu}^{m0} + 3\alpha_{\lambda\mu}^{m0}\bar{\alpha}_{\lambda\mu} + 3\alpha_{\lambda\mu}^{m0}\bar{\alpha}_{\mu\lambda}^{m0}\Big)D$$
$$+\Big(\alpha_{\lambda\lambda}^{m0}\bar{\alpha}_{\mu\mu}^{m0} + \alpha_{\lambda\mu}^{m0}\bar{\alpha}_{\lambda\mu}^{m0} + \alpha_{\lambda\mu}^{m0}\bar{\alpha}_{\mu\lambda}^{m0}\Big)E\Big]. \tag{15}$$

which gives for the TPA B-coefficient

$$B_{\text{3D-LG(circ)}}^{(2)} = \frac{1}{240\hbar^2 c\varepsilon_0^2}\Bigg[\Big(-2\alpha_{\lambda\lambda}^{m0}\bar{\alpha}_{\mu\mu}^{m0} + 3\alpha_{\lambda\mu}^{m0}\bar{\alpha}_{\lambda\mu}^{m0} + 3\alpha_{\lambda\mu}^{m0}\bar{\alpha}_{\mu\lambda}^{m0}\Big)\frac{f^4}{2}$$
$$+\Big(-2\alpha_{\lambda\lambda}^{m0}\bar{\alpha}_{\mu\mu}^{m0} + 3\alpha_{\lambda\mu}^{m0}\bar{\alpha}_{\lambda\mu}^{m0} + 3\alpha_{\lambda\mu}^{m0}\bar{\alpha}_{\mu\lambda}^{m0}\Big)\frac{D}{2}$$
$$+\Big(\alpha_{\lambda\lambda}^{m0}\bar{\alpha}_{\mu\mu}^{m0} + \alpha_{\lambda\mu}^{m0}\bar{\alpha}_{\lambda\mu}^{m0} + \alpha_{\lambda\mu}^{m0}\bar{\alpha}_{\mu\lambda}^{m0}\Big)\frac{E}{2}\Bigg]. \tag{16}$$
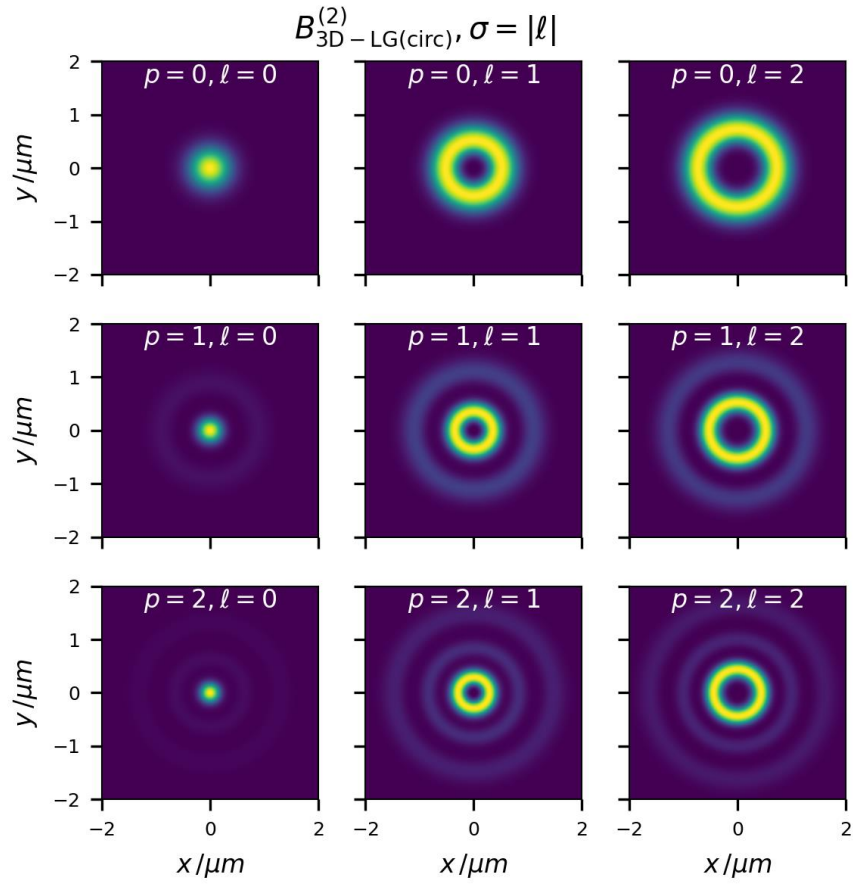
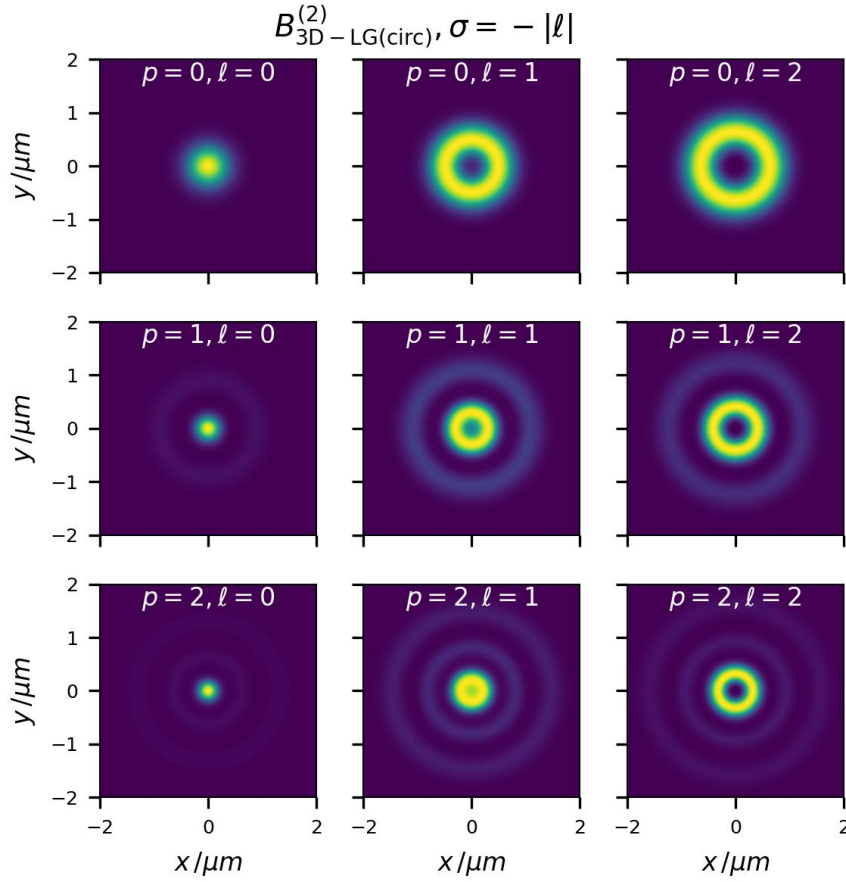**Figure 3:** Equation (16) for parallel spin angular momentum (SAM) and OAM. $w_0 = \lambda$.

Figure 4: Equation (16) for antiparallel SAM and OAM. $w_0 = \lambda$.

Using (11) we can decompose (16) into its irreducible components:

$$B_{\text{3D-LG(circ)}}^{(2)} = \frac{1}{240\hbar^2 c \varepsilon_0^2} \left[\frac{5}{6} E \alpha_{\lambda\lambda}^{(0)} \bar{\alpha}_{\mu\mu}^{(0)} + \left(3f^4 + 3D + E \right) \alpha_{\lambda\mu}^{(2)} \bar{\alpha}_{\lambda\mu}^{(2)} \right], \tag{17}$$

where D and E are given in Table 1. Again, it is helpful to compare (17) to the essentially plane wave case of a paraxial circularly polarized LG mode:

$$B_{\text{2D-LG(circ)}}^{(2)} = \frac{1}{240\hbar^2 c \varepsilon_0^2} 3\alpha_{\lambda\mu}^{(2)} \bar{\alpha}_{\lambda\mu}^{(2)} f_{|\ell|,p}^4. \tag{18}$$
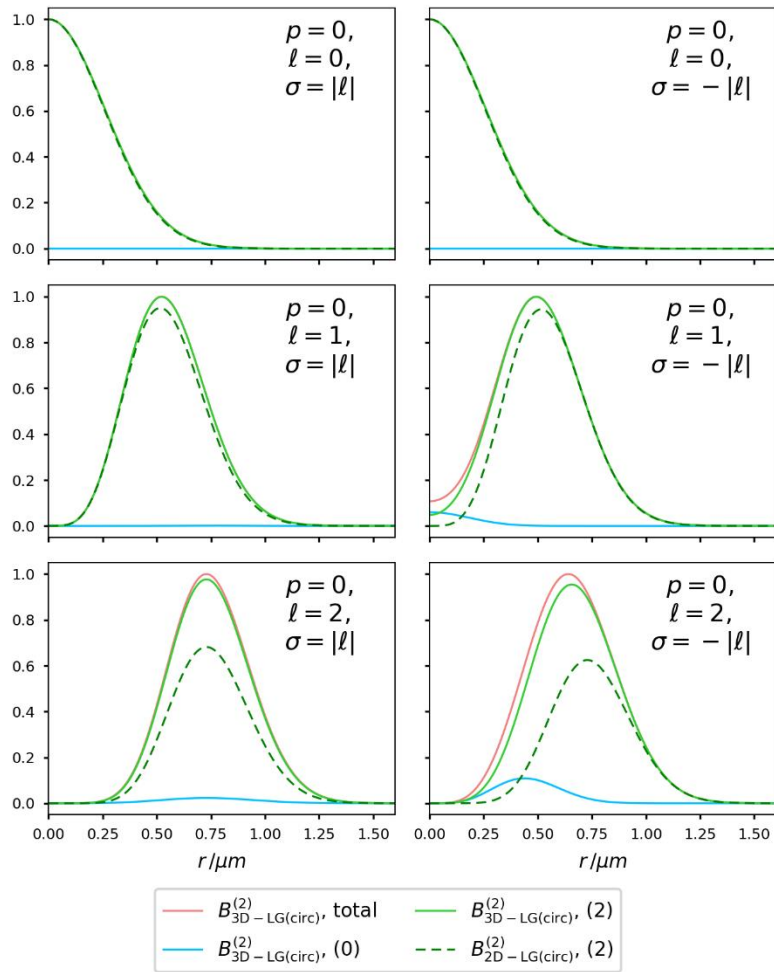
Figure 5: Irreducible tensor analysis of 3D LG mode (17) TPA (solid lines) versus 2D LG mode (18) (dashed lines). Left hand side shows the case of parallel SAM and OAM; right hand side shows antiparallel SAM and OAM. $p = 0$, $w_0 = \lambda$.
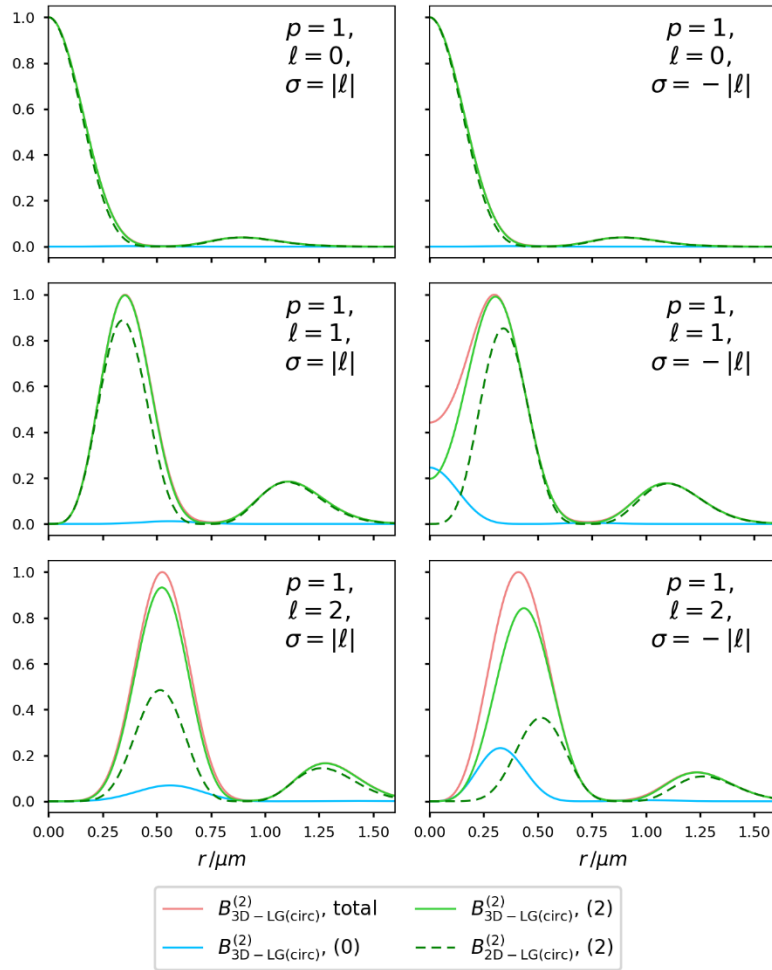
Figure 6: Irreducible tensor analysis of 3D LG mode (17) TPA (solid lines) versus 2D LG mode (18) (dashed lines). Left hand side shows the case of parallel SAM and OAM; right hand side shows antiparallel SAM and OAM. $p = 1$, $w_0 = \lambda$.
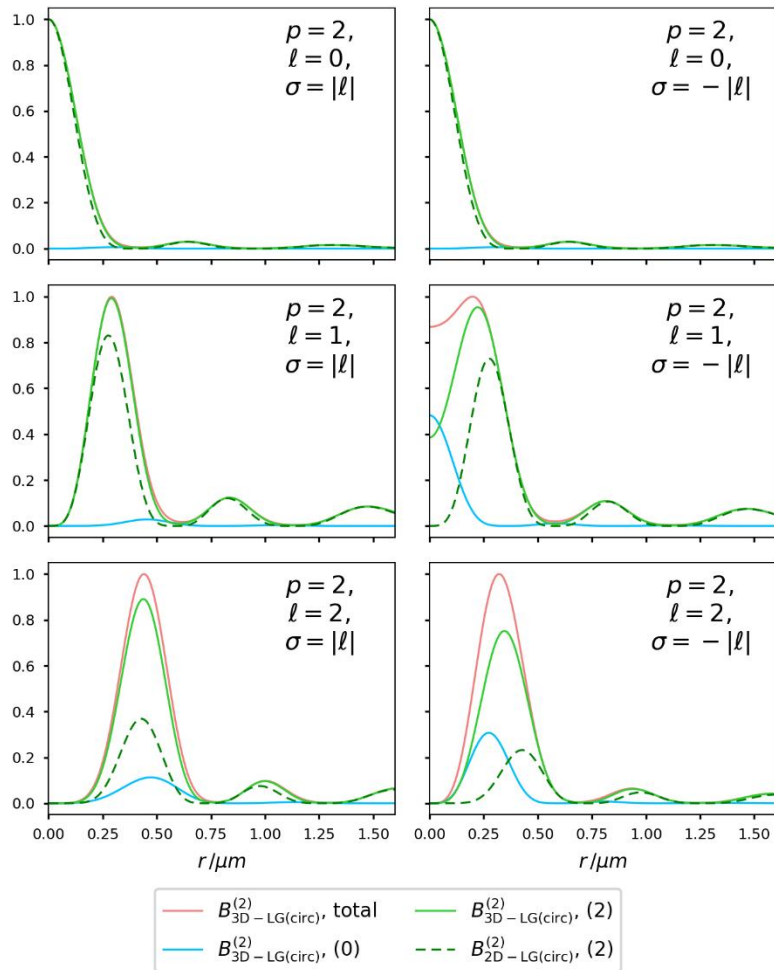
Figure 7: Irreducible tensor analysis of 3D LG mode (17) TPA (solid lines) versus 2D LG mode (18) (dashed lines). Left hand side shows the case of parallel SAM and OAM; right hand side shows antiparallel SAM and OAM. $p = 2$, $w_0 = \lambda$.

Remarkably, compared to the plane wave description (18), for the tightly focused fields (17) we produce non-zero weight 0 scalar absorption for a light source which is circularly polarized in a 2D sense (as also shown in Figures 5-7). The physical reason behind this is that in non-paraxial fields there is a spin-to-orbit angular momentum conversion, and the weight 0 term in (17) is proportional to the factor E which is a contribution that stems purely from the longitudinal fields that possess no integral SAM. Figures 5-7 highlight how this result constitutes a position-dependent selection rule in the electric dipole approximation. Further, the weight 0 contribution is larger for the anti-parallel case of SAM and OAM than it is for the parallel case, with the peak being on axis for $\pm|\sigma| = \mp|\ell|$. There is also a shift in the peak maximum for the anti-parallel 3D case compared to the 2D case, and this reflects the tighter focus which is possible in this scenario.

5. CONCLUSION

We have undertaken a systematic study of TPA from a tightly focused optical vortex. Compared to the well-known plane wave result[10], for a 3D structured optical vortex with 2D linear polarization there are small differences but generally the relative contributions from the irreducible molecular polarizability components are the same. However, in the case of a 3D

structured optical vortex with 2D circular polarization, there is a weight 0 contribution which does not occur in TPA carried out with plane wave excitation. This work constitutes the foundations of looking at how 3D structured light can probe matter in new ways compared to currently prevailing method of using plane wave and paraxial optical sources.

REFERENCES

1. He, G. S., Tan, L.-S., Zheng, Q. & Prasad, P. N. Multiphoton absorbing materials: molecular designs, characterizations, and applications. *Chem. Rev.* **108**, 1245–1330 (2008).

2. Zipfel, W. R., Williams, R. M. & Webb, W. W. Nonlinear magic: multiphoton microscopy in the biosciences. *Nat. Biotechnol.* **21**, 1369–1377 (2003).

3. Rumi, M. & Perry, J. W. Two-photon absorption: an overview of measurements and principles. *Adv. Opt. Photonics* **2**, 451–518 (2010).

4. Hayat, A., Nevet, A., Ginzburg, P. & Orenstein, M. Applications of two-photon processes in semiconductor photonic devices: invited review. *Semicond. Sci. Technol.* **26**, 083001 (2011).

5. Forbes, A., de Oliveira, M. & Dennis, M. R. Structured light. *Nat. Photonics* **15**, 253–262 (2021).

6. Shen, Y. *et al.* Optical vortices 30 years on: OAM manipulation from topological charge to multiple singularities. *Light Sci. Appl.* **8**, 1–29 (2019).

7. Allen, L., Beijersbergen, M. W., Spreeuw, R. J. C. & Woerdman, J. P. Orbital angular momentum of light and the transformation of Laguerre-Gaussian laser modes. *Phys. Rev. A* **45**, 8185–8189 (1992).

8. Andrews, D. L., Bradshaw, D. S., Forbes, K. A. & Salam, A. Quantum electrodynamics in modern optics and photonics: tutorial. *JOSA B* **37**, 1153–1172 (2020).

9. Woolley, R. G. Power-Zienau-Woolley representations of nonrelativistic QED for atoms and molecules. *Phys. Rev. Res.* **2**, 013206 (2020).

10. Craig, D. P. & Thirunamachandran, T. *Molecular Quantum Electrodynamics: An Introduction to Radiation-Molecule Interactions*. (Courier Corporation, 1998).

11. Forbes, K. A., Green, D. & Jones, G. A. Relevance of longitudinal fields of paraxial optical vortices. *J. Opt.* **23**, 075401 (2021).

12. Andrews, D. L. & Thirunamachandran, T. On three-dimensional rotational averages. *J. Chem. Phys.* **67**, 5026–5033 (1977).

13. Andrews, D. L. & Webb, B. S. Two-photon photoselection: an irreducible tensor analysis. *J. Chem. Soc. Faraday Trans.* **86**, 3051–3066 (1990).